photonics

MDPI

Article

A Theoretical Investigation of an Ultrawide S-, C- and L-Band-Tunable Random Fiber Laser Based on the Combination of Tellurite Fiber and Erbium-Doped Fiber

Lu Chen, Yang Li, Houkun Liang and Han Wu *

College of Electronics and Information Engineering, Sichuan University, Chengdu 610064, China; 2022222055215@stu.scu.edu.cn (L.C.); li.yang@scu.edu.cn (Y.L.); hkliaang@scu.edu.cn (H.L.)
* Correspondence: hanwu@scu.edu.cn

Abstract: In this paper, we present a new scheme to generate ultrawide tunable random fiber lasers (RFLs) covering the S-, C- and L-band by combining the broadband Raman gain in tellurite fibers and the active gain in erbium-doped fibers. A numerical simulation based on the power-balance model is conducted to verify the feasibility of the ultrawide tunable random fiber lasing generation. Pumped by a 1450 nm laser, the tunable random Raman fiber laser in the ranges of 1480–1560 nm and 1590–1640 nm can only be realized with a tellurite fiber. To further fill in the emission gap in the range of 1560–1590 nm, the erbium-doped fiber is incorporated in the cavity, which can provide efficient erbium-doped gain in the C- and L-band. By combining a 100 m long tellurite fiber and an 8 m long erbium-doped fiber, an ultrawide tunable RFL based on hybrid erbium–Raman gain can be realized with a wavelength tuning range (1480 nm–1640 nm) covering the S-, C- and L-band at 3.5 W pump power. Such a widely tunable RFL is of great importance in applications such as optical communication, sensing and imaging.

Keywords: random fiber laser; Rayleigh backscattering; tellurite fiber; hybrid gain

check for updates

Citation: Chen, L.; Li, Y.; Liang, H.; Wu, H. A Theoretical Investigation of an Ultrawide S-, C- and L-Band-Tunable Random Fiber Laser Based on the Combination of Tellurite Fiber and Erbium-Doped Fiber. *Photonics* **2024**, *11*, 247. https://doi.org/10.3390/photonics11030247

Received: 6 February 2024
Revised: 4 March 2024
Accepted: 6 March 2024
Published: 11 March 2024

Copyright: © 2024 by the authors. Licensee MDPI, Basel, Switzerland. This article is an open access article distributed under the terms and conditions of the Creative Commons Attribution (CC BY) license (https://creativecommons.org/licenses/by/4.0/).

1. Introduction

Wavelength-tunable fiber lasers operating in the communication band have been widely used in optical fiber communication, optical device testing and optical sensor systems over the past few decades [1–3]. The common way to achieve wavelength-tunable lasing is by incorporating a filter inside the laser cavity and utilizing rare-earth-doped fibers, such as erbium-doped fibers (EDFs), Thulium-doped fibers and Holmium-doped fibers. Tunable fiber lasers based on erbium-doped fiber have concentrated lots of attention extensive development thanks to their low threshold and high optical signal-to-noise ratio [4]. However, they can only generate emissions at a specific wavelength range located in the gain spectra of rare-earth-doped fibers. Another way to generate wavelength-agile tunable fiber lasers is by adopting nonlinear effects such as stimulated Raman scattering (SRS) as the gain mechanism. The Raman fiber laser successfully avoids the disadvantages mentioned above by being available at arbitrary wavelengths across the transparency window of the fiber and having high power and a simpler cavity configuration [5,6]. However, conventional Raman fiber lasers use pairs of gratings to provide feedback, which set a limitation of wavelength tunability. Random fiber lasers (RFLs) with a tunable wavelength emission do not depend on the cavity or the wavelength-selective devices and are therefore more suitable for the broadband lasing emission.

Since the random fiber laser, which is based on random Rayleigh scattering along single-mode fibers (SMFs), was proposed and demonstrated for the first time, it has garnered lots of attention and undergone tremendous development in recent years [7]. This novel kind of fiber laser has favorable stability and directionality, making it a promising

light source for optical communication, imaging sensing, nonlinear frequency conversion and high-output power applications [8–14].

Since the RFL utilizes distributed Rayleigh backward scattering as feedback, this unique cavity provides a new platform for wavelength-tunable fiber lasers with simple cavity configurations. The wavelength-tunable Raman RFL with a tuning range of 1535–1570 nm was first realized by incorporating tunable filters inside the cavity [15], which can achieve excellent power uniformity across the tuning range. Rare-earth-doped RFLs with tunable spectra have also been reported in erbium-doped RFLs [16,17] and ytterbium-doped RFLs [18,19] with low thresholds. The hybrid gain is further used to extend the wavelength tunability performance of RFLs. By adopting the hybrid Er-Raman gain, 1525–1603 nm random lasing can be realized with a forward pump structure [20–22]. Another way to generate widely tunable RFLs is through the combination of tunable pump lasers and cascaded Raman lasing [23–27]. In addition, nearly octave wavelength-tunable RFLs covering a 1–1.9 μm region have been realized by pump wavelength tuning and cascaded Raman shifting, whereas the S-, C- and L-band lasing requires a sixth- to eighth-order cascaded Raman process which requires a high threshold and for which it is difficult to control the lasing bandwidth due to the use of a broadband reflector [23–29]. On the other hand, the glass hosts (tellurite and bismuth oxide-based glasses) with high refractive indexes have been considered for expanding the gain bandwidth and the tunable range of fiber lasers. Among these, the tellurite fiber (TF), with remarkable properties, including a strong Raman gain coefficient, large Raman shift and broadband Raman gain spectrum, has been proven to realize ultrawide Raman amplification [30] and an ultrawide wavelength tuning range of the Raman laser [31]. Although a 160 nm wide flat gain was demonstrated in a tellurite-based fiber Raman amplifier [30], the researchers used multiple wavelength pump sources (1410, 1420, 1430 and 1460 nm pumps). Here, we try to explore the possibility of realizing ultrawide flat lasing generation with only one wavelength pump by introducing a hybrid erbium–Raman gain. Besides, high power output in the mid-infrared region and multi-wavelength generation based on tellurite fibers have also been reported [32–34]. Moreover, broadband erbium-doped tellurite fiber amplifiers in the 1.5 μm region have proven successful [35,36]. However, for the above-mentioned works based on the tellurite fiber, the tuning range was less than 100 nm with milliwatt-level output power, which requires improvement. We increase the tuning range in this paper while simultaneously enhancing the output power.

In this work, an ultrawide tunable RFL is proposed and theoretically investigated for the first time, based on the combination of broadband Raman gain in TFs and active gain in EDFs. A numerical simulation based on the power-balance model is conducted to verify the feasibility of the ultrawide tunable random fiber lasing generation. When the pump wavelength is fixed at 1450 nm, a tunable random Raman fiber lasing covering the ranges of 1480–1560 nm and 1590–1640 nm can only be realized with a tellurite fiber. To further fill in the emission gap in the range of 1560–1590 nm, the EDF is incorporated in the cavity, which can provide efficient erbium-doped gain in the C- and L-bands. Eventually, we elaborately analyze the optimized pump power of 3.5 W, EDF length of 8 m and TF length of 100 m, at an ultrawide tuning range from 1470 to 1640 nm, which covers the S-, C- and L-bands with optimized flatness random lasing which can be realized based on hybrid erbium–Raman gain. To the best of our knowledge, this is the widest tuning range ever reported for first-order random Raman fiber lasers.

2. Principle and the Numerical Modeling

The proposed scheme of the tunable RFL is shown in Figure 1a. The 1450 nm pump source is injected into the laser cavity through a wavelength-division multiplexer (WDM; pass port: 1450 nm, reflection port: 1480–1650 nm). The combination of an 8 m long EDF (EDFC-980-HP, Nufern, East Granby, CT, USA) and a 100 m long tellurite fiber (TF) is used as the gain medium. The EDF can provide erbium-doped gain pumped by a 1450 nm laser and the TF can provide broadband Raman gain. Besides, the random Rayleigh

backscattering inside the TF can provide random distributed feedback. In order to realize wavelength tunability, the reflection port of the WDM is connected to a 1:1 coupler-based fiber loop mirror that incorporates a tunable filter to provide the wavelength-selectable point feedback. The output port of TF is cleaved to minimize the backward reflection. With the help of hybrid erbium–Raman gain, the wavelength-selectable point feedback and the random Rayleigh distributed feedback, random fiber lasing can be generated in the half-open cavity and the wavelength can be tuned by tuning the central wavelength of the tunable filter.

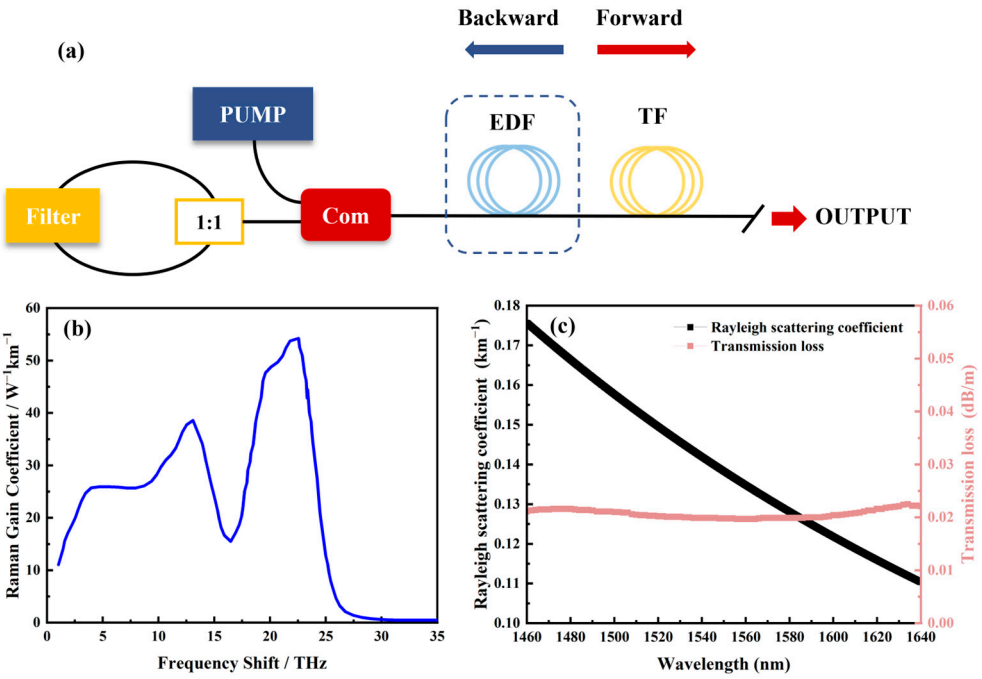


Figure 1. (**a**) Proposed scheme of the tunable RFL. WDM, wavelength-division multiplexer; EDF, erbium-doped fiber; TF, tellurite fiber; (**b**) Raman gain coefficients of the tellurite fiber used in the simulation; (**c**) Rayleigh scattering coefficient and transmission loss of the tellurite fiber used in the simulation.

The Raman gain coefficient of the tellurite fiber used in the simulation is shown in Figure 1b [31]. A peak value for the Raman gain coefficients of 55 W^{-1} km^{-1} is obtained for this tellurite fiber, while the corresponding Raman shift is around 22.3 THz. The first-order Stokes is estimated to be 1625 nm with a Raman shift of ~175 nm when the pump wavelength is 1450 nm and the Raman gain profile of the TF is relatively broad, which shows its potential for constructing a widely tunable Raman RFL covering the S-, C- and L-bands. Figure 1c presents the Rayleigh scattering coefficient and transmission loss of the tellurite fiber used in the simulation from 1460 nm to 1640 nm, which are referred to in Refs. [31,37]. It is worth mentioning that the transmission loss of tellurite fiber used in this paper, which is produced only by the Toyota Technological Institute in the Yasutake Ohishi group (20 dB/km), is significantly lower than most experimental and commercial tellurite fibers (at levels $\geq$ 300 dB/km).

We established the power-balance model by considering both the Raman gain in the TF and the erbium-doped gain in the EDF, respectively. The main factors considered in the section TF are fiber transmission loss, Rayleigh backscattering and Raman gain. To theoretically analyze and optimize the performance of the RFL, the power evolution of the pump and the first Stokes in forward propagation in the TF can be calculated by Equations (1)–(3) below.

$$\frac{dP_k^{\pm}}{dz} = \mp\alpha_k P_k^{\pm} \pm \eta g_k (P_0^{+} + P_0^{-})(P_k^{\pm} + 0.5\Gamma_k) \pm \varepsilon_k P_k^{\pm} \mp (1-\eta)\sum_{k'=1}^{N} \frac{v_0}{v_{k'}}(P_{k'}^{+} + P_{k'}^{-} + \Gamma_{k'})P_0^{\pm} \quad (1)$$

$$\Gamma_k = 4hv_k\Delta v_{ks}\left(1 + \frac{1}{\exp[h(v_0 - v_k)/(k_B T)] - 1}\right) \tag{2}$$

$$\varepsilon = \frac{3}{16}\frac{n_1^2 - n_2^2}{n_1^2}\alpha_s = \frac{3}{8}\triangle n\alpha_s \tag{3}$$

In this model, the superscripts '+' and '−' denote the transmission direction of forward and backward propagation of pump and Stokes waves, respectively. Subscript '*k*' represents the light waves with the *k*-th calculated wavelength. α_k, ν_k, ε_k and g_k represent the attenuation coefficient, frequency, Rayleigh scattering coefficient and Raman gain coefficient of the corresponding wavelength, respectively. Γ_k is the population of phonon which corresponds to the spontaneous Raman scattering. $\Delta\nu_{ks}$ is the lasing bandwidth. T stands for the absolute temperature of 298 K, k_B is Boltzmann's constant and h is Plank's constant. Equation (3) shows the Rayleigh backscattering coefficient, ε, as a function of the refractive indices, n_1 and n_2, with a refractive index difference, Δn, of 2.2% and a scattering loss, α_s, which is approximately 20–40% of the total loss [30,31,37].

In this section of the EDF, Rayleigh backscattering could be neglected due to the short length of the EDF. We calculate the power evolution through the Giles model [20].

$$\frac{dP_k^{\pm}}{dz} = \pm(\alpha_k^* + g_k^*)\frac{\overline{n}_2}{\overline{n}_t}P_k^{\pm} \pm 2g_k^*\frac{\overline{n}_2}{\overline{n}_t}hv_k\Delta v_{ke} \mp (\alpha_k^* + l_k)P_k^{\pm} \tag{4}$$

$$\frac{\overline{n}_2}{\overline{n}_t} = \frac{\sum_{k=0}^{N}\frac{(P_k^+ + P_k^-)\alpha_k^*}{hv_0\zeta}}{1 + \sum_{k=0}^{N}\frac{(P_k^+ + P_k^-)(\alpha_k^* + g_k^*)}{hv_k\zeta}} \tag{5}$$

$\alpha^*{}_k$ and $g^*{}_k$ represent the absorption coefficient and gain coefficient provided by Nufern (EDFC-980-HP). $\bar{n}_2$ denotes the erbium ion population of the upper energy level and $\bar{n}_t$ denotes the total erbium ion population of the ground state and the upper energy levels. ν_k and $\Delta\nu_{ke}$ denote the light frequency and the noise bandwidth separately. l_k (=0.01 dB/m) is the background loss and ζ (=3.87 × 10^{15} m^{-1} s^{-1}) is the saturation parameter.

To solve this model, the following boundary conditions, in which L is the total length of two fibers and R is the reflectivity at the filter end, should be satisfied.

$$\begin{cases} P_1(L) = 0 \\ R{\cdot}P_1^-(0) = P_1^+(0) \\ P_0^+(0) = P_0 \end{cases} \tag{6}$$

The parameters used for representing the output power as a function of pump power of TF are summarized in Table 1 [31,37].

Table 1. Fiber parameters in the numerical simulation.

Wavelength (nm)	ε (m^{-1})	g ($W^{-1}km^{-1}$)	α (dB/km)
1480	1.67×10^{-5}	26	21.6
1550	1.38×10^{-5}	36.4	20
1580	1.28×10^{-5}	17.8	19.9
1640	1.10×10^{-5}	32.6	22.1

3. Results

In the simulation, the reflectivity of the coupler-based fiber loop mirror and the parasitic reflection are set to 0.95 and 0.00001, respectively. As for the spectrum, the wavelength interval for calculating interpolation is 1 nm. To show the advantage of the combination of TFs and EDFs for broader wavelength tuning range, we numerically calculate the lasing wavelength tuning spectra with and without EDFs.

First, we calculate the situation of tunable RFLs with TFs only. Figure 2a shows the output power of different wavelengths as a function of pump power when the TF length is set to 100 m. The thresholds of 1480 nm, 1550 nm and 1640 nm are approximately 2.2 W, 1.6 W and 1.8 W, respectively. When the threshold is exceeded, the output power increases rapidly with the increase in pump power. The output power can reach 2.01 W, 2.03 W and 1.88 W of 1480 nm, 1550 nm and 1640 nm random lasing at 3.5 W of pump power. However, the 1580 nm Stokes component has not been stimulated due to the relatively low corresponding Raman gain coefficient pumped by 1450 nm. Figure 2b shows the effect of TF length. The laser threshold is higher when the length of the TF is relatively short because Rayleigh scattering needs to be accumulated over a long fiber. The fact that the shorter fiber length contributes to higher output power should be explained by the lower propagation loss. Therefore, the output powers of the 100 m TF and the 150 m TF are 2.01 W and 1.49 W, respectively, when the pump power is 3.5 W. The wavelength-tunable spectra are shown in Figure 2c with 3.5 W of pump power and a 100 m TF. The lasing in the range of 1560–1590 nm cannot be stimulated due to the low Raman gain coefficients in this range. Nevertheless, the tunable RFL with a flat amplitude can be realized in the 1480–1560 nm and 1590–1640 nm ranges, which verifies the significant advantages in tunability by using a TF as the Raman fiber. The output powers as a function of lasing wavelengths at different pump powers, when the TF length is fixed as 100 m, are shown in Figure 2d. When the wavelength tuning range becomes broader with an increase in pump power and at 3.5 W of pump power, the wide tuning range with excellent power flatness can be achieved. It should also be noted that second-order Raman lasing is not considered in this work due to the high threshold of >4 W.

To fill in the emission gap in the range of 1560–1590 nm, the EDF is incorporated in the cavity, which can provide efficient erbium-doped gain in the 1560–1590 nm range, then the random lasing can be generated based on the hybrid erbium–Raman gain pumped by 1450 nm. Figure 3 shows the RFL performances with the combination of an 8 m EDF and a 100 m TF. The lasing emission spectra are shown in Figure 3a at 3.5 W of pump power. A continuous tuning range of 160 nm from 1480 nm to 1640 nm is realized by using this laser cavity structure, which covers the S-, C- and L-bands. Figure 3b shows the output power at different wavelengths as a function of pump power. Among them, the 1580 nm random lasing, which has not been stimulated with the TF alone, is also stimulated by the combination of EDFs and TFs with a lower threshold of about 1.6 W. Moreover, the power of 1550 nm random lasing increases rapidly with about only a 100 mW threshold which is because strong erbium-doped gain can significantly reduce the lasing threshold. With 3.5 W of pump power, the output powers of 1480 nm, 1550 nm, 1580 nm and 1640 nm are 1.97 W, 1.95 W, 1.83 W and 1.84 W, respectively. Since hybrid gain of EDFs and TFs provides a lower threshold, the 1480 nm lasing can be stimulated more effectively than the TF-only configuration with the same pump power. In addition, a lower loss of TFs at 1480 nm can also contribute to the higher output power of 1480 nm than the other three wavelengths, which also contributes to the higher efficiency of 1480 nm lasing beyond the threshold shown in Figure 2a. Figure 3c shows output powers of the tunable wavelength RFL at different pump powers. At a relatively low pump power, the output power of 1580 nm lasing is lower; however, the uniformity of power distribution gradually improves with the increase in pump power and excellent power uniformity in the range of 1480–1640 nm can be realized at a pump power of 3.5 W.

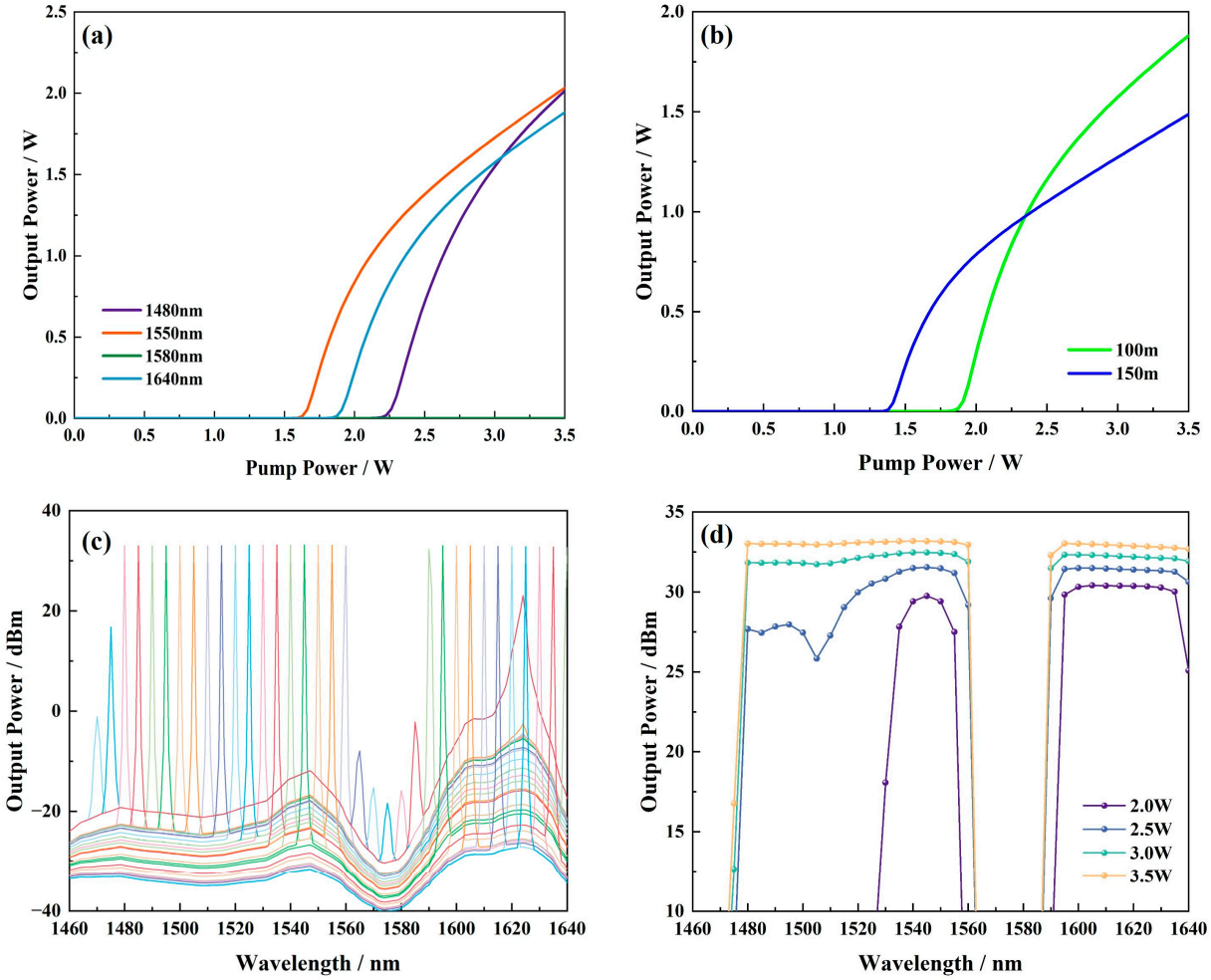


Figure 2. Output power as a function of pump power (**a**) for the lasing wavelengths of 1480 nm, 1550 nm, 1580 nm and 1640 nm and (**b**) for the TFs of length 100 m and 150 m. (**c**) Tunable lasing spectra when the pump power is fixed at 3.5 W. (**d**) Output powers as a function of lasing wavelength at pump powers of 2.0 W, 2.5 W, 3.0 W and 3.5 W.

Finally, we compare the effects of different lengths of EDFs. As shown in Figure 4a, when the EDF length is only 4 m, there is still an emission gap near 1580 nm due to the insufficient erbium-dope gain. However, when the length of the EDF is beyond 8 m, continuous tunable lasing from 1480 to 1640 nm can be achieved with good uniformity. Figure 4b shows the variation in the 1580 nm output power with the increase in pump power with different EDF lengths in detail. For the lengths of 8 m and 12 m, the thresholds are 1.51 W and 0.31 W, respectively, and the output powers are 1.88 W and 1.93 W, respectively, at 3.5 W of pump power. Since the output power performance is nearly unchanged with the increase in EDFs for the wavelengths that are located outside the erbium-doped gain regime (such as 1480 nm and 1640 nm), by considering pump power at 3.5 W, the output power flatness of the 8 m EDF is similar to that of the 12 m EDF, so we choose the length of EDF as 8 m in the simulation for Figure 3.

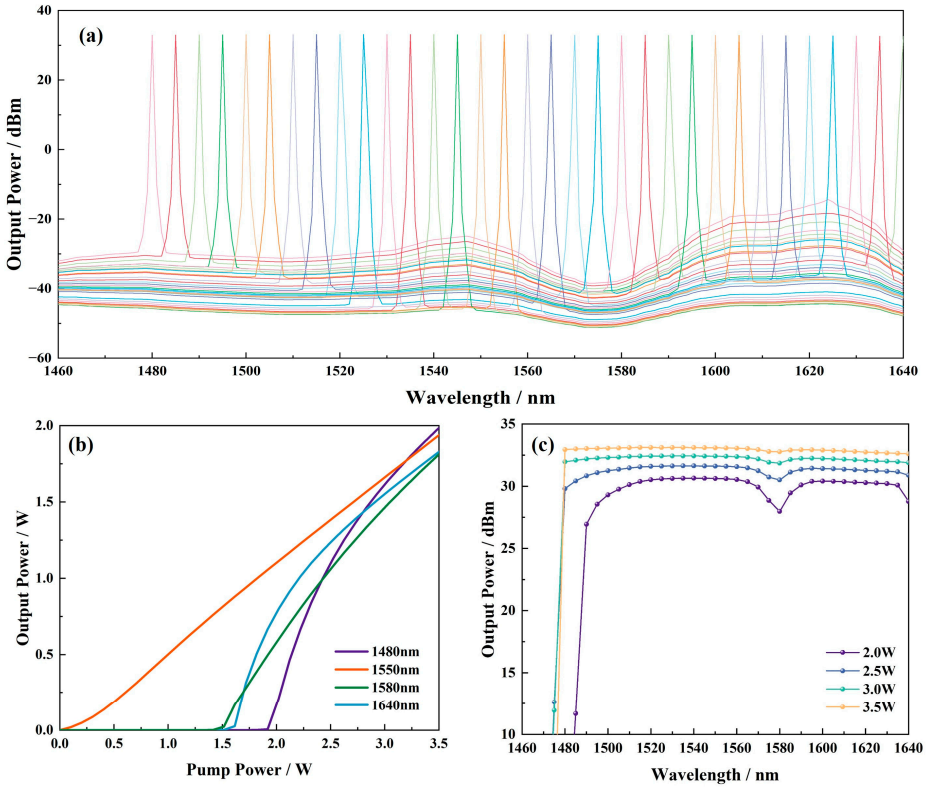


Figure 3. (**a**) Emission spectra of the tunable RFL with the combination of EDFs and TFs when the pump power is fixed at 3.5 W. (**b**) Output powers as a function of pump powers for the lasing wavelengths of 1480 nm, 1550 nm, 1580 nm and 1640 nm. (**c**) Output powers as a function of lasing wavelengths at pump powers of 2.0 W, 2.5 W, 3.0 W and 3.5 W.

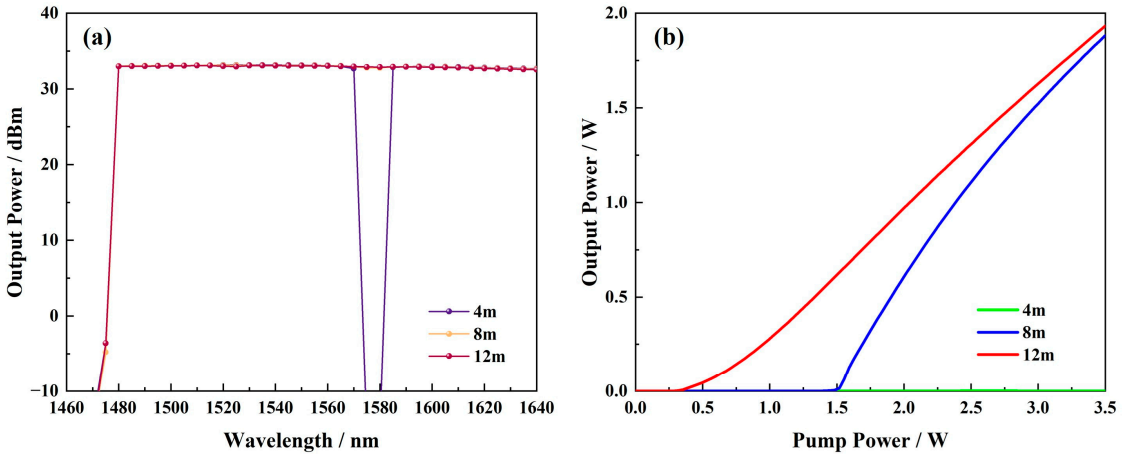


Figure 4. (**a**) Output powers as a function of lasing wavelengths for the cases of the EDFs of length 4 m, 8 m and 12 m (**b**) Output powers of 1580 nm lasing as a function of pump powers for the cases of the EDFs of length 4 m, 8 m and 12 m.

4. Discussion

Considering that the loss of commercial TF in most experiments is approximately 300 dB/km, we also performed a comparative calculation. The scattering loss is about 30% of the total loss and the backward Rayleigh scattering coefficients were calculated using Equation (3) [37]. With the much higher loss, to realize the random lasing, the length of the TF should be decreased with the need for much higher pump power. Figure 5a shows the output powers of different wavelengths as a function of the pump powers when the

TF length is set to 20 m. Similar to Figure 2a, the 1580 nm Stokes component has not been stimulated due to the low Raman gain coefficient. The thresholds of 1480 nm, 1550 nm and 1640 nm are about 16.2 W, 12 W and 13.7 W, respectively. The output powers increased rapidly with the pump power and reached 4.5 W, 5.1 W and 4.6 W of 1480 nm, 1550 nm and 1640 nm, respectively, at 22 W pump power. The effect of different lengths of the TFs is shown in Figure 5b. Similar to Figure 2b, by using a longer TF length of 30 m, although the threshold value of 12 W can be achieved, the efficiency is also much lower. On the other hand, the output power was only 3.5 W because the threshold was too high (20 W) with a 10 m long TF. The wavelength-tunable spectra are shown in Figure 5c with a 22 W pump power and a 20 m long TF. The lasing range of 1560–1590 nm cannot be stimulated due to the low Raman gain coefficient. Figure 5d shows the output power distribution of different wavelengths at pump powers of 16 W, 18 W, 20 W and 22 W. The widest tuning ranges of 1480–1560 nm and 1590–1640 nm were achieved at 22 W pump power.

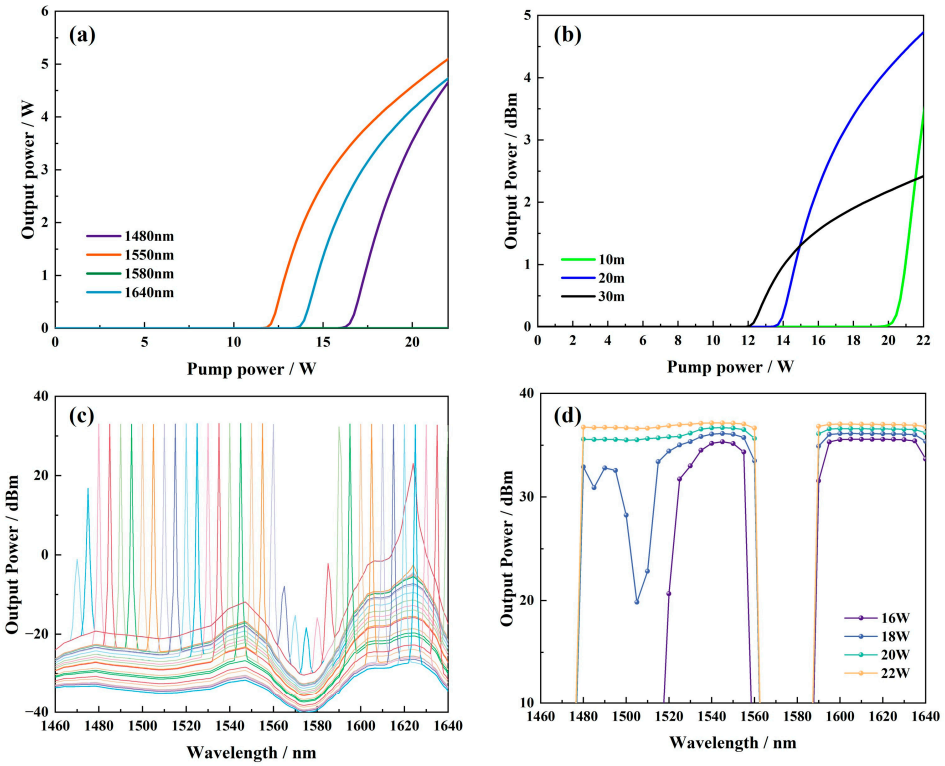


Figure 5. Output power as a function of pump power (**a**) for the lasing wavelengths of 1480 nm, 1550 nm, 1580 nm and 1640 nm and (**b**) for the TFs with lengths 10 m, 20 m and 30 m. (**c**) Tunable lasing spectra when the pump power is fixed at 22 W. (**d**) Output powers as a function of lasing wavelength at pump powers of 16 W, 18 W, 20 W and 22 W.

We also performed a new simulation with the combination of a 20 m long TF (300 dB/km) and an 8 m long EDF. Figure 6 shows the tunable spectra at a 22 W pump power. A tuning range of 160 nm from 1480 to 1640 nm with excellent uniformity was also achieved by the combination of EDFs and TFs, which covers the S-, C- and L-bands. It should be noted that the high-power 1450 nm pump laser with more than 20 W output power is feasible, including the cascaded Raman fiber laser reported in [23].

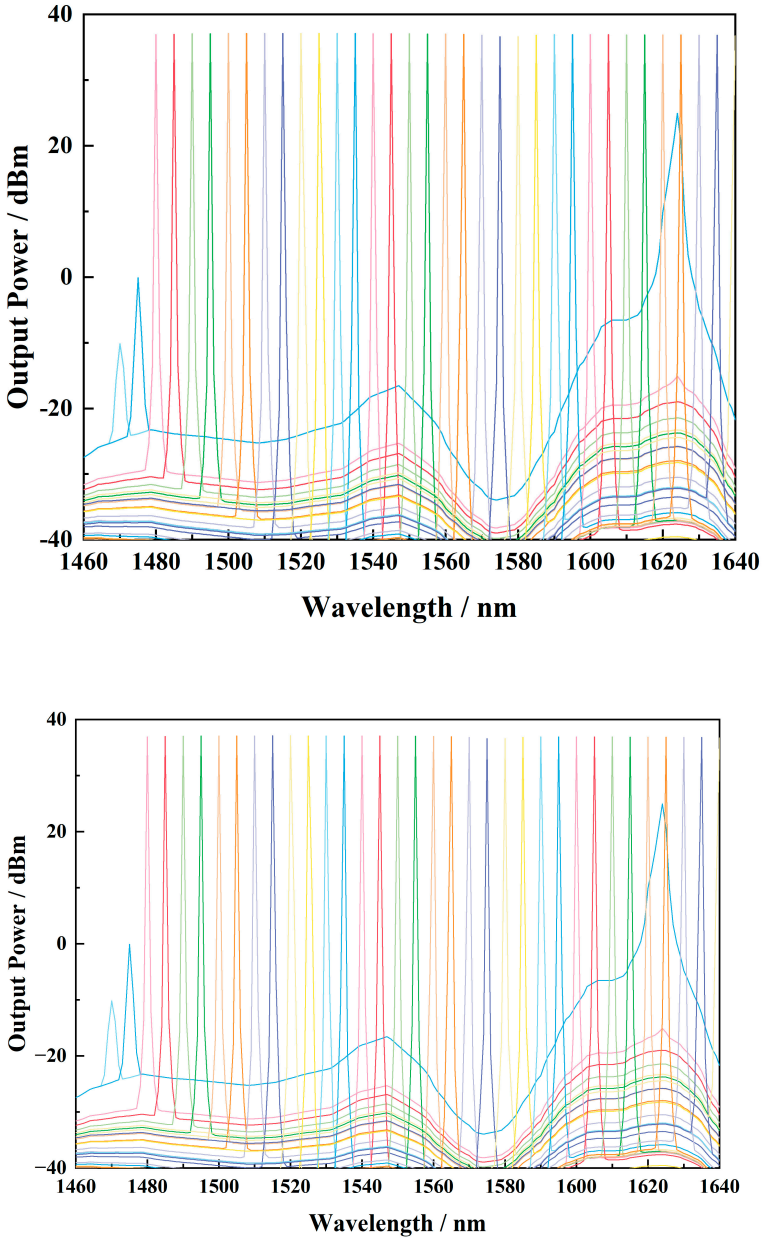


Figure 6. Emission spectra of tunable RFLs with the combination of EDFs and TFs when the pump power is fixed at 22 W.

5. Conclusions

In this paper, we have demonstrated a new scheme to generate an ultrawide tunable random fiber laser by a combination of tellurite fibers and erbium-doped fibers. A numerical simulation based on the power-balance model was conducted to verify the feasibility of the ultrawide tunable random fiber lasing generation. Tunable lasing covering 1480–1560 nm and 1590–1640 nm could only be achieved by tellurite fibers with a 1450 nm pump. To further extend the tuning range, the erbium-doped fiber was incorporated in the cavity, which provided efficient erbium-doped gain in the C- and L-band. Eventually, by combining Raman gain in the 100 m long tellurite fiber and erbium-doped gain in the 8 m long erbium-doped fiber, an ultrawide random fiber laser with a continuous tuning range (1480–1640 nm) covering the S-, C- and L-bands could be realized at 3.5 W pump power, which could provide an effective method for optimizing a widely tunable RFL in technologies like optical communication, device testing and sensor systems.

Author Contributions: L.C. and Y.L. did the numerical modeling, L.C. and H.W. analyzed the data, L.C., H.W. and H.L. wrote this paper. All authors have read and agreed to the published version of the manuscript.

Funding: National Natural Science Foundation of China (62005186, 62005187), Sichuan Provincial Department of Science and Technology (2022YFSY0049).

Data Availability Statement: The data underlying the results presented in this article are not publicly available at this time but may be obtained from the authors upon reasonable request.

Conflicts of Interest: The authors declare no conflicts of interest.

References

1. Al-Taiy, H.; Wenzel, N.; Preußler, S.; Klinger, J.; Schneider, T. Ultra-Narrow Linewidth, Stable and Tunable Laser Source for Optical Communication Systems and Spectroscopy. *Opt. Lett.* **2014**, *39*, 5826–5829. [CrossRef] [PubMed]
2. Fu, Z.; Yang, D.; Ye, W.; Kong, J.; Shen, Y. Widely Tunable Compact Erbium-Doped Fiber Ring Laser for Fiber-Optic Sensing Applications. *Opt. Laser Technol.* **2009**, *41*, 392–396. [CrossRef]
3. Dong, B.; He, S.; Hu, S.; Tian, D.; Lv, J.; Zhao, Q. Time-Division Multiplexing Fiber Grating Sensor with a Tunable Pulsed Laser. *IEEE Photon. Technol. Lett.* **2006**, *18*, 2620–2622. [CrossRef]
4. Masson, J.; St-Gelais, R.; Poulin, A.; Peter, Y.-A. Tunable Fiber Laser Using a MEMS-Based in Plane Fabry-Pérot Filter. *IEEE J. Quantum Electron.* **2010**, *46*, 1313–1319. [CrossRef]
5. Supradeepa, V.R.; Feng, Y.; Nicholson, J.W. Raman Fiber Lasers. *J. Opt.* **2017**, *19*, 023001. [CrossRef]
6. Babin, S.A.; Churkin, D.V.; Kablukov, S.I.; Rybakov, M.A.; Vlasov, A.A. All-Fiber Widely Tunable Raman Fiber Laser with Controlled Output Spectrum. *Opt. Express* **2007**, *15*, 8438–8443. [CrossRef]
7. Turitsyn, S.K.; Babin, S.A.; El-Taher, A.E.; Harper, P.; Churkin, D.V.; Kablukov, S.I.; Ania-Castañón, J.D.; Karalekas, V.; Podivilov, E.V. Random Distributed Feedback Fibre Laser. *Nat. Photon* **2010**, *4*, 231–235. [CrossRef]
8. Tan, M.; Rosa, P.; Le, S.T.; Iqbal, M.A.; Phillips, I.D.; Harper, P. Transmission Performance Improvement Using Random DFB Laser Based Raman Amplification and Bidirectional Second-Order Pumping. *Opt. Express* **2016**, *24*, 2215–2221. [CrossRef]
9. Tian, M.; Zhang, W.; Huang, W. Review of Random Fiber Lasers for Optical Fiber Sensors. *Sensors* **2023**, *23*, 8500. [CrossRef]
10. Ma, R.; Wang, Z.; Hui Zhang, H.; Zhang, W.L.; Jiang Rao, Y. Imaging through Opacity Using a Near-Infrared Low-Spatial-Coherence Fiber Light Source. *Opt. Lett.* **2020**, *45*, 3816–3819. [CrossRef]
11. Wu, H.; Han, B.; Wang, Z.; Genty, G.; Feng, G.; Liang, H. Temporal Ghost Imaging with Random Fiber Lasers. *Opt. Express* **2020**, *28*, 9957–9964. [CrossRef] [PubMed]
12. Wu, H.; Wang, W.; Hu, B.; Li, Y.; Tian, K.; Ma, R.; Li, C.; Liu, J.; Yao, J.; Liang, H. Widely Tunable Continuous-Wave Visible and Mid-Infrared Light Generation Based on a Dual-Wavelength Switchable and Tunable Random Raman Fiber Laser. *Photonics Res.* **2023**, *11*, 808–816. [CrossRef]
13. Rota-Rodrigo, S.; Gouhier, B.; Dixneuf, C.; Antoni-Micollier, L.; Guiraud, G.; Leandro, D.; Lopez-Amo, M.; Traynor, N.; Santarelli, G. Watt-level green random laser at 532 nm by SHG of a Yb-doped fiber laser. *Opt. Lett.* **2018**, *43*, 4284–4287. [CrossRef] [PubMed]
14. Dontsova, E.I.; Kablukov, S.I.; Vatnik, I.D.; Babin, S.A. Frequency Doubling of Raman Fiber Lasers with Random Distributed Feedback. *Opt. Lett.* **2016**, *41*, 1439–1442. [CrossRef] [PubMed]
15. Babin, S.A.; El-Taher, A.E.; Harper, P.; Podivilov, E.V.; Turitsyn, S.K. Tunable Random Fiber Laser. *Phys. Rev. A* **2011**, *84*, 021805. [CrossRef]
16. Wang, L.; Dong, X.; Shum, P.P.; Su, H. Tunable Erbium-Doped Fiber Laser Based on Random Distributed Feedback. *IEEE Photonics J.* **2014**, *6*, 1–5. [CrossRef]
17. Li, Z.; He, W.; Zhang, W.; Liu, H.; Li, S.; Tan, Q.; Zhu, L. Wavelength tunable double-ring cavity erbium-doped random fiber laser based on a Mach–Zehnder interferometer. *Opt. Fiber Technol.* **2023**, *79*, 103337. [CrossRef]
18. Du, X.; Zhang, H.; Wang, X.; Zhou, P. Tunable Random Distributed Feedback Fiber Laser Operating at 1 μm. *Appl. Opt.* **2015**, *54*, 908–911. [CrossRef]
19. Wu, H.; Wang, W.; Li, Y.; Li, C.; Yao, J.; Wang, Z.; Liang, H. Difference-Frequency Generation of Random Fiber Lasers for Broadly Tunable Mid-Infrared Continuous-Wave Random Lasing Generation. *J. Light. Technol.* **2022**, *40*, 2965–2970. [CrossRef]
20. Wu, H.; Wang, Z.; Sun, W.; He, Q.; Wei, Z.; Rao, Y.-J. 1.5 μm Low Threshold, High Efficiency Random Fiber Laser with Hybrid Erbium–Raman Gain. *J. Light. Technol.* **2018**, *36*, 844–849. [CrossRef]
21. Bian, S.; Li, W.; Song, S. C- and L-Band Tunable Random Distributed Feedback Fiber Laser. In Proceedings of the 2016 Photonics North (PN), Quebec City, QC, Canada, 24–26 May 2016; p. 1.
22. Su, B.; Luo, Q.; Zhao, L.; Chu, L.; Wang, L.; Liu, C.; He, X. Optimization of Widely Tuneable Hybrid Erbium-Raman-Gain Random Fibre Laser: Theoretical Investigation. *J. Mod. Opt.* **2021**, *68*, 847–855. [CrossRef]
23. Balaswamy, V.; Aparanji, S.; Arun, S.; Ramachandran, S.; Supradeepa, V.R. High-Power, Widely Wavelength Tunable, Grating-Free Raman Fiber Laser Based on Filtered Feedback. *Opt. Lett.* **2019**, *44*, 279–282. [CrossRef] [PubMed]
24. Zhang, L.; Jiang, H.; Yang, X.; Pan, W.; Cui, S.; Feng, Y. Nearly-Octave Wavelength Tuning of a Continuous Wave Fiber Laser. *Sci. Rep.* **2017**, *7*, 42611. [CrossRef] [PubMed]

25. Balaswamy, V.; Ramachandran, S.; Supradeepa, V.R. High-Power, Cascaded Random Raman Fiber Laser with near Complete Conversion over Wide Wavelength and Power Tuning. *Opt. Express* **2019**, *27*, 9725–9732. [CrossRef]
26. Dong, J.; Zhang, L.; Jiang, H.; Yang, X.; Pan, W.; Cui, S.; Feng, Y. High order cascaded Raman random fiber laser with high spectral purity. *Opt. Express* **2018**, *26*, 5275–5280. [CrossRef]
27. Wu, H.; Han, B.; Liu, Y. Tunable Narrowband Cascaded Random Raman Fiber Laser. *Opt. Express* **2021**, *29*, 21539–21550. [CrossRef]
28. Zhang, Y.; Song, J.; Ye, J.; Xu, J.; Yao, T.; Zhou, P. Tunable Random Raman Fiber Laser at 17 μm Region with High Spectral Purity. *Opt. Express* **2019**, *27*, 28800–28807. [CrossRef]
29. Zhang, Y.; Ye, J.; Ma, X.; Xu, J.; Song, J.; Yao, T.; Zhou, P. High Power Tunable Multiwavelength Random Fiber Laser at 1.3 μm Waveband. *Opt. Express* **2021**, *29*, 5516–5524. [CrossRef]
30. Mori, A.; Masuda, H.; Shikano, K.; Shimizu, M. Ultra-Wide-Band Tellurite-Based Fiber Raman Amplifier. *J. Light. Technol.* **2003**, *21*, 1300–1306. [CrossRef]
31. Qin, G.; Liao, M.; Suzuki, T.; Mori, A.; Ohishi, Y. Widely Tunable Ring-Cavity Tellurite Fiber Raman Laser. *Opt. Lett.* **2008**, *33*, 2014–2016. [CrossRef]
32. Yao, T.; Huang, L.; Zhou, P.; Lei, B.; Leng, J.; Chen, J. Power Scaling on Tellurite Glass Raman Fibre Lasers for Mid-Infrared Applications. *High Power Laser Sci. Eng.* **2018**, *6*, e24. [CrossRef]
33. Zhu, G.; Geng, L.; Zhu, X.; Li, L.; Chen, Q.; Norwood, R.A.; Manzur, T.; Peyghambarian, N. Towards Ten-Watt-Level 3-5 μm Raman Lasers Using Tellurite Fiber. *Opt. Express* **2015**, *23*, 7559–7573. [CrossRef] [PubMed]
34. Anashkina, E.A.; Andrianov, A.V. Numerical Analysis of Dual-Wavelength Tungsten-Tellurite Fiber Raman Lasers with Controllable Mode Switching. *Fibers* **2023**, *11*, 84. [CrossRef]
35. Mori, A.; Sakamoto, T.; Kobayashi, K.; Shikano, K.; Oikawa, K.; Hoshino, K.; Kanamori, T.; Ohishi, Y.; Shimizu, M. 1.58-μm Broad-Band Erbium-Doped Tellurite Fiber Amplifier. *J. Light. Technol.* **2002**, *20*, 822–827. [CrossRef]
36. Ohishi, Y.; Mori, A.; Yamada, M.; Ono, H.; Nishida, Y.; Oikawa, K. Gain Characteristics of Tellurite-Based Erbium-Doped Fiber Amplifiers for 1.5-μm Broadband Amplification. *J. Opt. Lett.* **1998**, *23*, 274–276. [CrossRef]
37. Tian, Y.; Yao, T.; Zhou, P.; Zhang, H.; Leng, J.; Xu, J.; Chen, J. Numerical Modeling and Optimization of Mid-Infrared Random Distributed Feedback Fiber Lasers. *Laser Phys.* **2018**, *28*, 075104. [CrossRef]

Disclaimer/Publisher's Note: The statements, opinions and data contained in all publications are solely those of the individual author(s) and contributor(s) and not of MDPI and/or the editor(s). MDPI and/or the editor(s) disclaim responsibility for any injury to people or property resulting from any ideas, methods, instructions or products referred to in the content.